Measurement of Magnetic Fields Generated by a Lightning Current Flowing Through Reinforced Concrete Walls

Susana Naranjo Villamil, Julien Gazave, Eric Piedallu, Maud Franchet, Boris Marquois, Christophe Guiffaut, Alain Reineix

Measurement of Magnetic Fields Generated by a Lightning Current Flowing Through Reinforced Concrete Walls

Susana Naranjo Villamil
EDF Power Networks Lab
EDF Group
Moret-Loing-et-Orvanne, France
susana.naranjo-villamil@edf.fr

Julien Gazave
EDF Power Networks Lab
EDF Group
Moret-Loing-et-Orvanne, France
julien.gazave@edf.fr

Eric Piedallu
EDF Power Networks Lab
EDF Group
Moret-Loing-et-Orvanne, France
eric.piedallu@edf.fr

Maud Franchet
EDF Power Networks Lab
EDF Group
Moret-Loing-et-Orvanne, France
maud.franchet@edf.fr

Boris Marquois
EDF / DIPNN / DI / TEGG
EDF Group
Aix-En-Provence, France
boris.marquois@edf.fr

Christophe Guiffaut
CEM et Diffraction
Institut de recherche XLIM
Limoges, France
christophe.guiffaut@xlim.fr

Alain Reineix
CEM et Diffraction
Institut de recherche XLIM
Limoges, France
alain.reineix@xlim.fr

***Abstract*—Estimating the transient magnetic field generated by a direct lightning strike is essential to protect sensitive electronic devices in industrial facilities. The accuracy of the estimation depends on the approach and the representatives of the model. Out of the different alternatives available in the literature, the full-wave methods are usually the most reliable. Nevertheless, there is still uncertainty in the results because considering all the components of the electromagnetic environment in the models is virtually impossible. To validate the representation of reinforced concrete structures in full-wave simulations, in this paper, we compare the magnetic field measured between two interconnected reinforced concrete walls to the magnetic field computed using CST Studio Suite. Similar tendencies for the distribution of the peak-values are observed; yet, some adjustments may be necessary to reproduce the waveforms.**

***Index Terms*—lightning, magnetic field, reinforced concrete, measurements, industrial facility**

I. Introduction

To define protection measures against the Lightning Electromagnetic Pulse (LEMP) in industrial facilities, it is essential to estimate the magnetic field generated by a direct strike to a building. In industrial facilities, buildings are generally made of reinforced concrete, a combination of concrete and reinforcement, which is widely used in modern constructions. Moreover, when a building is struck by lightning, a high current flows along the lightning channel and through the reinforcement generating a transient electromagnetic field inside the building. This field can lead to an upset of electric installations and sensitive electronic devices nearby.

Typically, the reinforcement of the buildings consists of two interconnected layers of reinforcing grids, where cylindrical reinforcing steel bars (rebars) are arranged periodically to form square or rectangular meshes. Ideally, to estimate the transient magnetic field inside a building, one would have to consider all the components of the electromagnetic environment and carry out a full-wave simulation. A good estimation of the electromagnetic fields generated by a direct strike could be obtained using full-wave simulations, see e.g. [1]–[3]. However, the accuracy of the estimations depends on the representatives of the models, and due to our limited knowledge of the phenomenon, we have to make some hypotheses. Also, because of the complexity of the geometry of full-scale reinforced concrete buildings, simplifying the models is often necessary. This is when experiments play an important role. An experiment can be used to corroborate hypotheses and validate the representation of the main components of the electromagnetic environment in the model. A good agreement between measurements and computations of the magnetic field in reinforced concrete buildings has already been observed in [4]–[7].

In this paper, we present the magnetic field measured between two adjacent reinforced concrete walls when a current impulse is injected into their reinforcement. The measurement results are compared to the magnetic fields computed using two different solvers available in CST Studio Suite [8]. The first solver is based on the finite integration technique (FIT) [9] and the second on the transmission line matrix method (TLM) [10].

II. Experimental Setup

The measurements are performed at the testing facility of EDF TEGG. A scaled model of a reinforced concrete structure was built in the facility to study the different properties of commonly used materials in buildings. As shown in Fig. 1, the structure has two adjacent reinforced concrete walls over

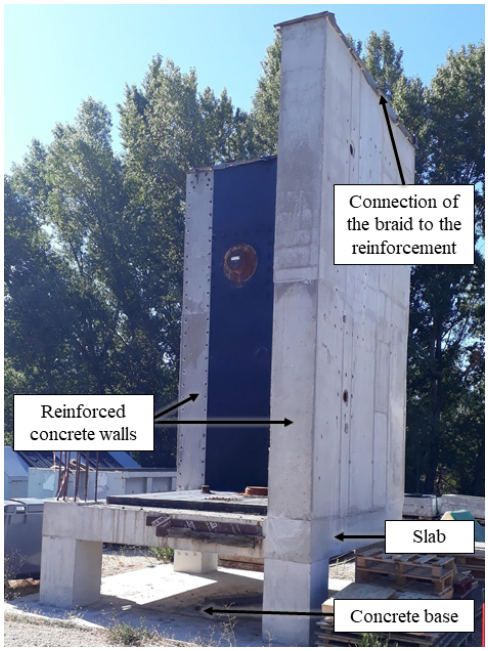

Fig. 1. Scaled model of the reinforced concrete structure at the testing facility of EDF TEGG.

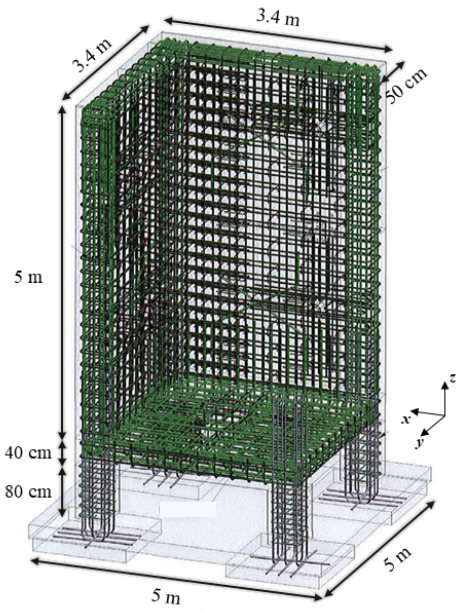

Fig. 2. Configuration of the reinforcement of the reinforced concrete walls and slab.

a reinforced concrete slab. The slab is supported by four symmetrical columns. In addition, there is a concrete base of 5 m $\times$ 5 m. The walls are 5 m in height, and their reinforcement is made up of a double-layered reinforcing grid embedded in 50 cm of concrete. The rebars of the reinforcing grid have a radius of 8 mm and form rectangular meshes of 20 cm $\times$ 25 cm. The layers are separated by 25 cm and interconnected every 50 cm.

The cross-sectional area of the slab is 3.4 m $\times$ 3.4 m. Its reinforcement is also made up of a double-layered reinforcing grid, with layers separated by 25 cm and interconnected every 50 cm. However, the reinforcing grid of the slab is embedded in 40 cm of concrete. Also, the rebars have radii of 8 mm and 10 mm and form square meshes of 25 cm $\times$ 25 cm. The columns supporting the slab are 1.2 m in height with a cross-sectional area of 50 cm $\times$ 50 cm. Out of the 1.2 m, only 80 cm are visible over the concrete base. The configuration of the reinforcement is shown in Fig. 2.

An IMU3000 test system [11] and a 25-meters-long copper braid are used to inject a current into the reinforcement of the walls. The copper braid is connected to the external layer of the reinforcement, at the top center of one of the walls. The IMU3000 simulates transients of different interference sources, including surge impulses as defined in the IEC 61000-4-5 standard [12]. At open-circuit it can generate a voltage impulse with a front time (T_m) of 1.2 μs and a time to half-value ($\Delta t_{50\%}$) of 50 μs. At short-circuit, it can generate a current impulse with a front time of 8 μs and a time to half-value of 20 μs. When using the IMU3000, the current injected into the reinforcement depends then on the load and therefore, on the experimental setup. The load could be approximated by

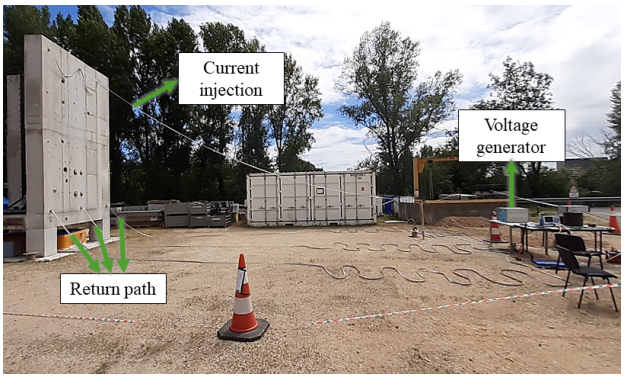

Fig. 3. Return path created using parallel braids in case A.

Fig. 4. Grounding point created for the generator in case B.

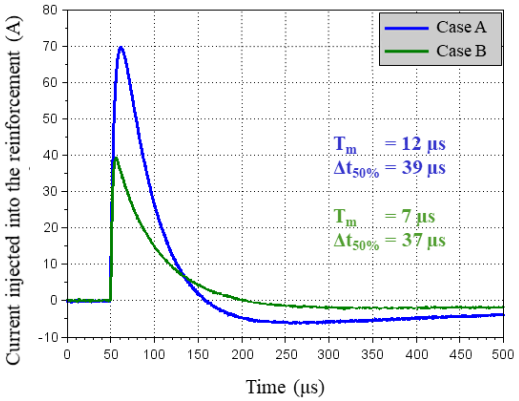

Fig. 5. Current injected into the reinforcement of the walls for an input voltage of 1 kV.

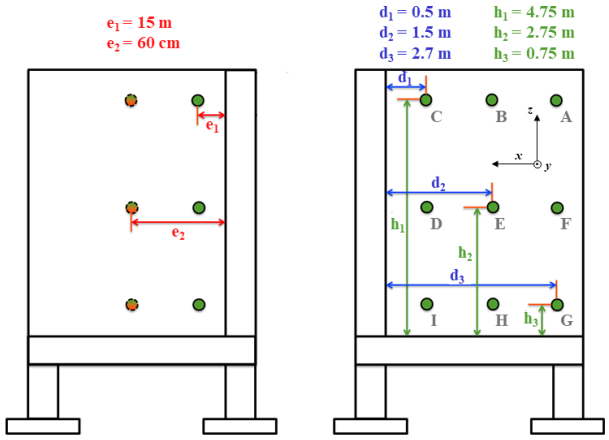

Fig. 6. Observation points.

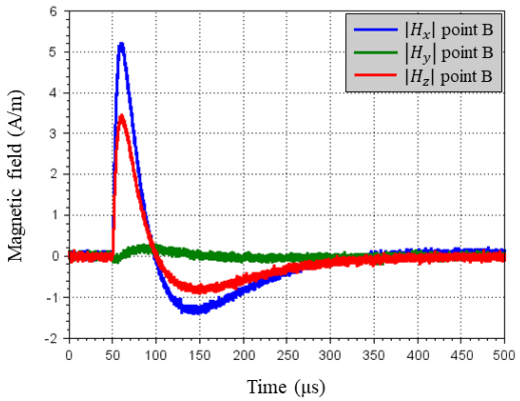

Fig. 7. Magnetic field measured in case A at 60 cm from the wall for an input voltage of 4 kV.

TABLE I
PEAK-VALUES OF THE X-COMPONENT OF THE MAGNETIC FIELDS MEASURED FOR AN INPUT VOLTAGE OF 4 KV

Point	Case A (A/m)		Case B (A/m)	
	30 cm	60 cm	30 cm	60 cm
A	6.0	4.3	4.6	4.1
B	6.9	5.1	7.2	4.7
C	4.9	4.5	4.4	4.3
D	1.6	1.7	1.6	1.8
E	4.6	4.0	4.4	3.7
F	15.2	7.3	9.3	5.9
G	14.9	6.6	11.1	7.1
H	4.5	4.0	5.0	4.7
I	1.2	1.7	2.1	2.2

adding up the impedance of the copper braid used to inject the current, the impedance of the structure, and the impedance of the return path. Two return paths are tested:

- Case A: Three parallel 25-meters-long copper braids are connected to the external layer of the reinforcement at the bottom of the wall and back to the generator (see Fig. 3). Note that to reduce the front time and the amplitude of the current injected into the reinforcement, a 10 Ω resistance is added in series with the copper braids.
- Case B: The 10 Ω resistance is removed and the soil is used as a return path. To do so, a grounding point had to be created for the generator. As shown in Fig. 4, the grounding point is a meshed network of 1 m × 1 m made of copper. It is buried at a depth of 1 m, 16 m away from the structure.

The impedance of the return paths is fundamentally different. The parallel braids have negligible resistance and high inductance; thus, the impedance of the return path in case A is mainly reactive. On the other hand, the soil has a limited conductivity and the inductance of the braid used to connect the generator to the grounding point is low; thus, the impedance of the return path in case B is mainly resistive. Accordingly, even though we had added a resistance in series with the braids in case A, the current injected in case B is lower and its front time is shorter (see Fig. 5).

We performed preliminary measurements varying the amplitude of the impulses generated with the IMU3000, and as expected, we did not observe significant changes in the current waveform. The current injected into the reinforcement was proportional to the voltage; hence, we set the voltage to 4 kV. As shown in Fig. 5, for a voltage of 1 kV, the maximum currents were about 70 A and 40 A for case A and case B, respectively. For a voltage of 4 kV, they were about 280 A and 160 A.

The magnetic field was measured at 9 points behind the wall, designated by letters A to I, using a custom-made unidirectional transducer with a sensitivity of 4 mV/(A·m^{-1}). There was only one transducer and it had to be moved and turned to measure point by point each component of the magnetic field separately. First, we measured the field at 30 cm and then at 60 from the wall; thus, there was a total of 18 observation points. As shown in Fig. 6, the points were distributed by combining the distance to the slab (h), the distance to the wall where the current was injected (e), and the

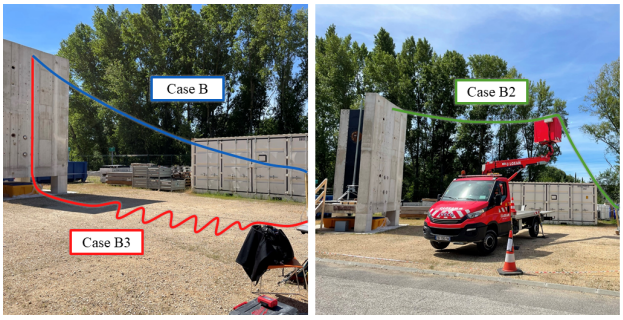

Fig. 8. Cases considered to study the influence of the angle between the wall and the braid used to inject the current into the reinforcement.

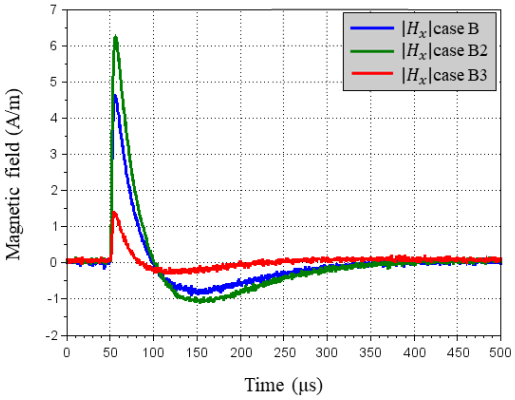

Fig. 9. Magnetic field measured for an input voltage of 4 kV when changing the angle formed by the wall and the braid used to inject the current.

distance to the adjacent wall (d). The voltage signals obtained using the transducer were amplified by 24 dB and optically transmitted to an oscilloscope, where they were recorded and saved.

III. Measurement Results

We started by measuring all the components of the magnetic field in case A and then decided to focus on the x-component (H_x). Since the current flows through the structure towards the ground, H_x is the most dominant component of the magnetic field (see e.g. Fig. 7). Table I summarizes the results.

As expected, the peak-values measured in case B are generally lower because the current injected into the reinforcement in case B is around 120 A less than the current injected in case A. However, the tendency is similar in both cases. The highest magnetic fields were measured close to the point where the current was injected (point B) and close to the external vertical edge (points A, F, and G). A higher magnetic field close to the external vertical edge could be explained by the current displacement phenomenon. It has been observed that when a reinforced concrete building is struck by lightning, the current is not uniformly distributed in the reinforcement, it is diverted to the edges [2], [3], [5].

It is also interesting to observe that at the points where the field is the highest (points F and G), the difference between the measurements at 30 cm and 60 cm is the biggest. On the contrary, the difference between the measurements at 30 cm and 60 cm is minor at points close to the adjacent wall (points C, D, and I). This could be explained by the superposition of the fields. The x-component of the magnetic fields generated by the flow of the currents in the walls goes in opposite directions. Thus, close to the adjacent wall, there is a higher compensation, i.e., the x-component of the magnetic field is lower, and the decay of the magnetic field with the distance is less visible. In addition, the results in Table I show that in case B, the magnetic field is higher close to the slab (points G, H, I) than in the middle of the wall (points D, E, and F), probably because in case B there is a higher current flowing through the slab and towards the opposite columns to go down to the ground. In case A, the current flowing through the slab is probably lower because of the parallel copper braids connected at the bottom of the wall.

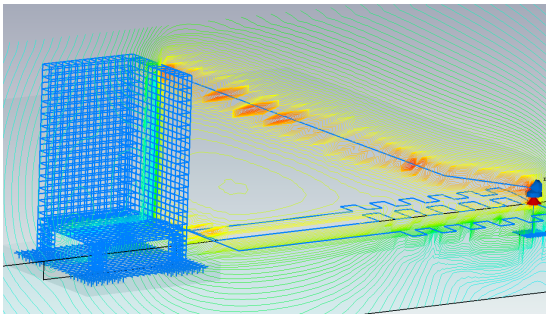

Fig. 10. Numerical model of the structure in case A.

To see if the experimental setup was affecting the results, after performing all the measurements, we changed the angle formed by the wall and the braid used to inject the current in case B. As shown in Fig. 8, we considered a case in which the angle is approximately 90°(case B2) and another in which it is 0° (case B3). Unsurprisingly, we observed that the angle had a significant influence on the results, especially at points B, E, and H. As an example, the results at point B are shown in Fig. 9. When the angle is less than 90°, there is again a compensation of the fields and therefore, the total field is lower. Ideally, the angle should be higher or equal to 90° to minimize the effect of the braid used to inject the current.

It is important to note that the results presented in this paper come straight from the measurements. Other than reducing the magnitude by 24 dB and using the sensibility of the transducer to convert from mV to A/m, signal processing has not been applied. We are working on estimating the calibration factor of the transducer and the measurement uncertainty to adjust the curves.

IV. Numerical Model

To validate the representation of the reinforcement in full-wave simulations, the magnetic fields at the 18 observation points in Fig. 6 are computed using CST Studio Suite [8], a software package for EM and multiphysics simulations. CST Studio Suite offers time domain and frequency domain solvers,

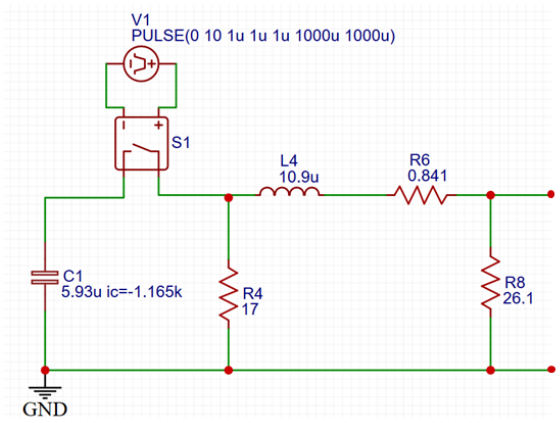

Fig. 11. Model of the combination wave generator implemented in CST Studio Suite.

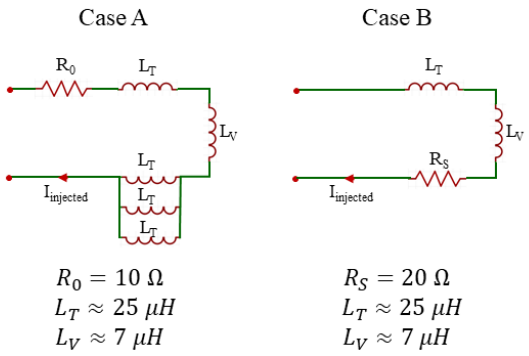

Fig. 12. Loads considered to verify the model of the combination wave generator.

from which we chose a solver based on the finite integration technique (FIT) [9] and a solver based on the transmission line matrix method (TLM) [10]. The FIT and the TLM are both similar to the FDTD method. One of their main differences comes from how they handle dielectric materials. A good comparison between the methods is presented by Laisné *et al.* in [13].

In CST Studio Suite, the reinforcement of the structure is modeled using perfectly conducting wires (see Fig. 10). The soil is considered homogeneous with a resistivity of 50 Ω·m, which is on average the resistivity we measured at the testing facility. In reality, the soil at the testing facility is not homogeneous. Using the Schlumberger method, we obtained values between 47 Ω·m and 56 Ω·m.

The IMU3000 test system is modeled as the combination wave generator suggested in [14]. Note that, as shown in Fig. 11, we made slight changes in the values of some of the circuit's components. The simplified circuit of the generator in Fig. 11 has also been recommended by the IEC 61000-4-5 standard [12], and it has previously been implemented to compare simulation and measurement results (see e.g. [15]).

To verify the current waveform before implementing the model in CST Studio Suite, we considered the simple representation of the load shown in Fig. 12. First, we included the resistance $R_0 = 10\ \Omega$ that had been added in series with the copper braids in case A. Then, we assumed that the braids have a linear inductance of 1 μH/m and no resistance; thus, $L_T \approx 25\ \mu$H. In addition, we measured the impedance of the structure using a vector network analyzer (VNA), which led to $L_V \approx 7\ \mu$H. Finally, based on the area and resistivity of the soil, we set the resistance of the return path $R_S \approx 20\ \Omega$ in case B. With these values and using PSpice [16], we obtained comparable currents. Nevertheless, in CST Studio Suite, the currents injected into the reinforcement still did not match the currents measured (see Fig. 13).

In case A, the peak-values of the currents obtained with different solvers are similar, yet, their time to half-value is shorter compared to the time to half-value of the current

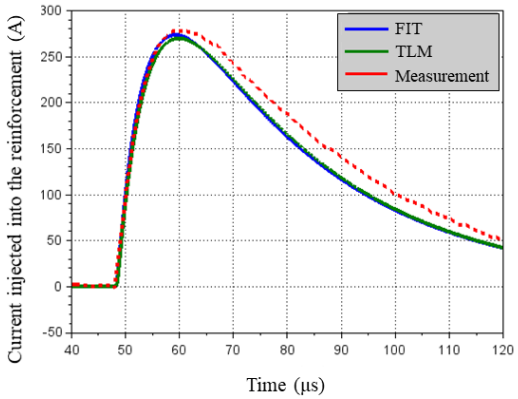

Fig. 13. Current injected into the reinforcement for an input voltage of 4 kV. (a) Case A. (b) Case B.

measured. In case B, using the solver based on the FIT, there is a significant error in both the front time ($\sim 20\%$ shorter) and the peak-value ($\sim 16\%$ higher), whereas using the solver based on the TLM, there is only a significant error in the peak-value ($\sim 15\%$ lower). As a result, there are discrepancies between the magnetic fields measured at the facility and the

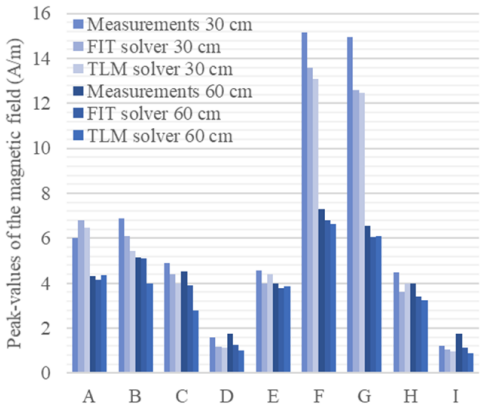

(a)

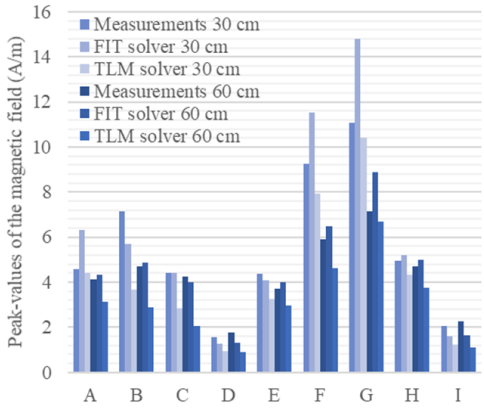

(b)

Fig. 14. Peak-values of the x-component of the magnetic fields computed using CST Studio Suite (a) Case A. (b) Case B.

magnetic fields computed using CST Studio Suite (see Fig. 14). In case A, the computations with different solvers result in similar peak-values of the magnetic field. The error between the computations and the measurements is about 2 dB on average. On the other hand, the error between the computations and the measurements can go up to 6 dB in case B. On the bright side, the tendencies observed in the magnetic field measured at the facility are also observed in the magnetic field computed using both solvers. Thus, by adjusting the model of the generator and applying the calibration factor of the transducer, we could expect to reduce the error significantly.

V. Conclusion

This paper presented the magnetic field measured at a scaled model of a reinforced concrete structure at the testing facility of EDF TEGG. We observed that, as expected, the x-component of the magnetic field is the most dominant, and the braid used to inject the current affects the results.

The highest peak-values of the field were measured close to the point where the current was injected and close to the external vertical edge. Similar tendencies were followed by the magnetic fields computed using CST Studio Suite. Yet, there was a non-negligible error in the peak-values. On average, the error between the computations and the measurements was lower when using the FIT solver. However, there were observation points at which the results obtained with the TLM solver were always in better agreement with the measurements. Hence, we cannot yet recommend a solver for future computations. To reduce the error and make a recommendation, it will be necessary to adjust the model of the generator and apply signal processing to the measurement results.

References

[1] A. Tatematsu, F. Rachidi, and M. Rubinstein, "Analysis of electromagnetic fields inside a reinforced concrete building with layered reinforcing bar due to direct and indirect lightning strikes using the FDTD method," *IEEE Transactions on Electromagnetic Compatibility*, vol. 57, no. 3, pp. 405–417, Jun. 2015. [Online]. Available: http://ieeexplore.ieee.org/document/7047933/

[2] I. Metwally and F. Heidler, "Reduction of lightning-induced magnetic fields and voltages inside struck double-layer grid-like shields," *IEEE Transactions on Electromagnetic Compatibility*, vol. 50, no. 4, pp. 905–912, Nov. 2008. [Online]. Available: http://ieeexplore.ieee.org/document/4663118/

[3] S. Naranjo-Villamil, C. Guiffaut, J. Gazave, and A. Reineix, "Lightning-induced magnetic fields inside grid-like shields: An improved formula complemented by a polynomial chaos expansion," *IEEE Transactions on Electromagnetic Compatibility*, vol. 63, no. 2, pp. 558–570, 2021.

[4] W. Zischank, F. Heidler, J. Wiesinger, I. Metwally, A. Kern, and M. Seevers, "Laboratory simulation of direct lightning strokes to a modeled building: measurement of magnetic fields and induced voltages," *Journal of Electrostatics*, vol. 60, no. 2-4, pp. 223–232, Mar. 2004. [Online]. Available: https://linkinghub.elsevier.com/retrieve/pii/S0304388604000257

[5] I. Metwally, W. Zischank, and F. Heidler, "Measurement of magnetic fields inside single- and double-layer reinforced concrete buildings during simulated lightning currents," *IEEE Transactions on Electromagnetic Compatibility*, vol. 46, no. 2, pp. 208–221, May 2004. [Online]. Available: http://ieeexplore.ieee.org/document/1300761/

[6] A. Kern, F. Heidler, M. Seevers, and W. Zischank, "Magnetic fields and induced voltages in case of a direct strike—comparison of results obtained from measurements at a scaled building to those of IEC 62305-4," *Journal of Electrostatics*, vol. 65, no. 5-6, pp. 379–385, May 2007. [Online]. Available: https://linkinghub.elsevier.com/retrieve/pii/S0304388606001197

[7] T. Maksimowicz and K. Aniserowicz, "Investigation of models of grid-like shields subjected to lightning electromagnetic field: experiments in the frequency domain," *IEEE Transactions on Electromagnetic Compatibility*, vol. 54, no. 4, pp. 826–836, Aug. 2012. [Online]. Available: http://ieeexplore.ieee.org/document/6093958/

[8] Dassault Systèmes, "CST Studio Suite," Vélizy-Villacoublay Cedex, France.

[9] T. Weiland, "Finite Integration Method and Discrete Electromagnetism," in *Computational Electromagnetics*, P. Monk, C. Carstensen, S. Funken, W. Hackbusch, and R. H. W. Hoppe, Eds. Berlin, Heidelberg: Springer Berlin Heidelberg, 2003, pp. 183–198.

[10] W. Hoefer, "The transmission-line matrix method - theory and applications," *IEEE Transactions on Microwave Theory and Techniques*, vol. 33, no. 10, pp. 882–893, 1985.

[11] *Immunity Tests: IMU3000 Test System*, EMC PARTNER, Sep. 2013.

[12] International Electrotechnical Commission (IEC), "IEC 61000-4-5: Electromagnetic compatibility (EMC) – Part 4-5: Testing and measurement techniques – Surge immunity test," 2014.

[13] A. Laisné and J. Drouet, "Comparison of finite integration technique (fit) and transmission line matrix (tlm) for numerical dosimetry in hf/vhf band," in *2013 International Symposium on Electromagnetic Compatibility*, 2013, pp. 659–664.

[14] International Telecommunication Union (ITU), "ITU-T K.44: Resistibility tests for telecommunication equipment exposed to overvoltages and overcurrents – Basic Recommendation," 2019.

[15] X. Pan, T. Rinkleff, B. Willmann, and R. Vick, "Pspice simulation of surge testing for electrical vehicles," in *International Symposium on Electromagnetic Compatibility - EMC EUROPE*, 2012, pp. 1–6.

[16] Artedas France SARL, "PSpice," Saint-Maur, France.